Article

Sharp Melting Transitions in DNA Hybrids without Aggregate Dissolution: Proof of Neighboring-Duplex Cooperativity

Julianne M. Gibbs-Davis, George C. Schatz, and SonBinh T. Nguyen

J. Am. Chem. Soc., **2007**, 129 (50), 15535-15540 • DOI: 10.1021/ja073034g

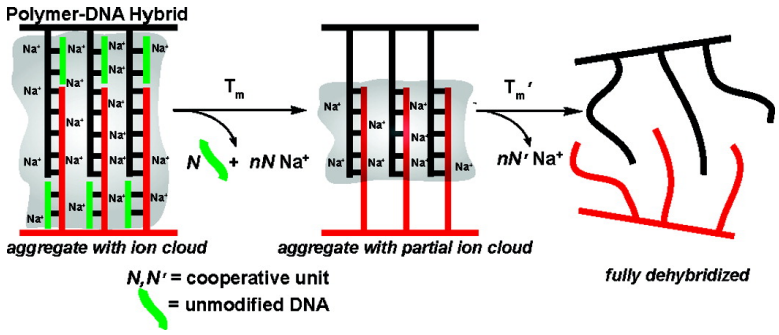

More About This Article

Additional resources and features associated with this article are available within the HTML version:

- Supporting Information
- Links to the 4 articles that cite this article, as of the time of this article download
- Access to high resolution figures
- Links to articles and content related to this article
- Copyright permission to reproduce figures and/or text from this article

View the Full Text HTML

J|A|C|S
ARTICLES
Published on Web 11/21/2007

Sharp Melting Transitions in DNA Hybrids without Aggregate Dissolution: Proof of Neighboring-Duplex Cooperativity

Julianne M. Gibbs-Davis, George C. Schatz,* and SonBinh T. Nguyen*

Contribution from the Department of Chemistry and International Institute for Nanotechnology, Northwestern University, 2145 Sheridan Road, Evanston, Illinois 60208-3113

Received May 9, 2007; Revised Manuscript Received July 17, 2007; E-mail: schatz@chem.northwestern.edu; stn@northwestern.edu

Abstract: Similar to DNA-modified gold nanoparticles, comb polymer−DNA hybrids exhibit very sharp melting transitions that can be utilized in highly selective DNA detection systems. Current theories suggest that such sharp melting results from either a phase transition caused by the macroscopic dissolution of the aggregate or neighboring-duplex interactions in the close-packed environment between adjacent DNA duplexes. To delineate the contributions of each of these effects, an aggregate system based on polymer−DNA hybrids was designed to include both polymer-linked and partially untethered duplexes. When this hybridized system was subjected to thermal analysis, both types of duplexes exhibited sharp melting transitions. The very sharp melting transition displayed by the partially untethered DNA duplexes offers proof that neighboring-duplex interactions can indeed induce cooperativity. Contributions of this neighboring-duplex effect, as well as the enhanced stabilization observed in polymer−DNA:polymer−DNA aggregates, can be quantitatively assessed using a simple thermodynamic model. While neighboring-duplex interactions alone can lead to cooperative melting, the enhanced stabilization observed in polymer−DNA aggregates is a function of both neighboring-duplex interactions and multivalent or aggregate properties.

Introduction

Directed-assembly based on biomolecular recognition events is the cornerstone methodology employed in a wide range of disciplines such as DNA and protein detection,[1] DNA-templated synthesis,[2] molecular motors,[3] and molecular electronics.[4] However, controlling the assembly process, particularly the fidelity (i.e., selectivity) of the recognition element, remains challenging for many systems. In DNA detection, low probe selectivity can make it difficult to perform certain types of assays like single nucleotide polymorphism (SNP) analysis, where a target DNA strand with a single mutation must be easily discriminated from another analyte without the mutation. One attractive way to increase the selectivity in DNA detection strategies is to utilize DNA-modified materials that exhibit very sharp dissociation or melting transitions, which allow for temperature-based SNP discrimination. In this respect, DNA-modified gold nanoparticles[5−7] and comb polymer−DNA hybrids[8,9] both exhibit very sharp, switch-like melting properties and have been shown to be very selective detection probes when used in SNP analysis.[5,8] Each of these DNA-modified materials contains multiple DNA strands per structure and readily forms large, highly cooperative DNA duplex-linked aggregates when combined with its complementary analogue.

Previously we have shown that the enhanced melting temperatures and sharp, highly cooperative melting transitions in comb polymer−DNA hybrids are directly related to the presence of multiple DNA strands on the polymer backbone.[8] Interestingly, these sharp melting transitions were not observed in hybridization mixtures composed of polymer−DNA hybrids and unmodified DNA strands.[8] Only when polymer−DNA hybrids were hybridized with other polymer−DNA hybrids containing multiple DNA strands did the resulting melting profile exhibit both an increased melting point and a sharp transition. These results suggested that a network, or aggregate, of duplexes between the complementary multiply linked polymer−DNA was necessary for inducing the enhanced melting behavior. However, other DNA-based materials such as dendrimer−DNA hydrids have not exhibited sharp melting transitions despite the presence of multiple strands on each dendrimer.[10] In this latter system, increasing the number of DNA strands per structure only led to increased melting temperatures but not sharp (i.e., noncooperative) transitions.[10] To elucidate possible cooperative mechanisms for DNA melting, herein we report a novel polymer−DNA hybridization system where contributions to the melting transitions can be quantitatively delineated.

(1) Rosi, N. L.; Mirkin, C. A. *Chem. Rev.* **2005**, *105*, 1547−1562.
(2) Kanan, M. W.; Rozenman, M. M.; Sakurai, K.; Snyder, T. M.; Liu, D. R. *Nature* **2004**, *431*, 545−549.
(3) Kinbara, K.; Aida, T. *Chem. Rev.* **2005**, *105*, 1377−1400.
(4) Dupraz, C. J. F.; Nickels, P.; Beierlein, U.; Huynh, W. U.; Simmel, F. C. *Superlattices Microstruct.* **2004**, *33*, 369−379.
(5) Park, S.-J.; Taton, T. A.; Mirkin, C. A. *Science* **2002**, *295*, 1503−1506.
(6) Taton, T. A.; Lu, G.; Mirkin, C. A. *J. Am. Chem. Soc.* **2001**, *123*, 5164−5165.
(7) Taton, T. A.; Mirkin, C. A.; Letsinger, R. L. *Science* **2000**, *289*, 1757−1760.
(8) Gibbs, J. M.; Park, S.-J.; Anderson, D. R.; Watson, K. J.; Nguyen, S. T.; Mirkin, C. A. *J. Am. Chem. Soc.* **2005**, *127*, 1170−1178.
(9) Watson, K. J.; Park, S. J.; Nguyen, S. T.; Mirkin, C. A. *J. Am. Chem. Soc.* **2001**, *123*, 5592−5593.
(10) Shchepinov, M. S.; Mir, K. U.; Elder, J. K.; Frank-Kamenetskii, M. D.; Southern, E. M. *Nucleic Acids Res.* **1999**, *27*, 3035−3041.

Scheme 1. Hybridization of Complementary Polymer−DNA Hybrids **polyDNA(T_{10}-I)** and **polyDNA(T_{10}-II)** Leads to an Aggregate of Duplexes[a]

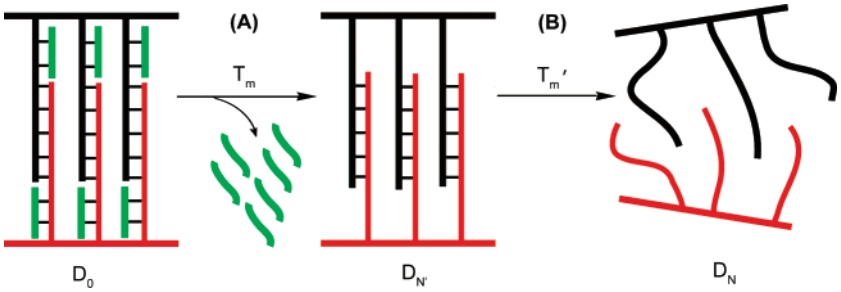

[a] The T_{10} spacer sequence between the complementary sequence and the polymer backbone is available for hybridization to a small A_{10} strand. (A) As the temperature is raised, the A_{10} strands first melt from the fully aggregated system (D_N) leaving the aggregate intact ($D_{N'}$). (B) At a higher temperature, the aggregate ($D_{N'}$) completely dissociates (D_0).

A complete understanding of the parameters that govern cooperativity in DNA hybrids would have broad ramifications. This understanding not only can influence probe design for DNA diagnostics but also may lead to breakthroughs in the general field of self-assembly. To this end, a significant amount of theoretical work has focused on determining the origin of the sharp behavior transitions observed for DNA-modified gold nanoparticles.[11−15] A major conjecture describes this melting as essentially a transition from a gel-like phase of the hybridized aggregate to a liquid phase of dehybridized components,[11−14] where the sharpness is related to the entropic cooperativity of the phase transition.[13] As such, any material that induces aggregation via a reversible process would exhibit switch-like dissociation behavior. Based on this principle, reversible polymer-based materials derived from hydrogen-bonding[16] and coordination-assembly[17] chemistry could be engineered for new detection systems. For example, using small-molecule targets to trigger the aggregation of reversible polymers in a highly selective manner would be an excellent approach to small-molecule detection.

However, a recent model reported by Jin et al. has attributed the sharp melting transitions observed for DNA-modified gold nanoparticles to specific short-range (<5 nm[15]) neighboring-duplex interactions between DNA duplexes within the aggregate.[18] In this theory, the close proximity of the charged DNA duplexes causes them to share a condensed cation cloud, leading to cooperative melting.[18] The insights from this conjecture allow us to incorporate a new parameter into the design of any material with applications that rely on the molecular recognition properties of DNA. Creating materials that arrange DNA such that neighboring strands can stabilize each other in a highly cooperative dielectric environment (i.e., the shared cation cloud) could allow other DNA-based materials to be incorporated into truly selective detection systems or utilized in other areas such as DNA-templated syntheses.[19,20]

Using polymer−DNA hybrids, we aim to delineate which theory, or combination of theories, best describes the origins of sharp melting in DNA-based materials. Our polymer−DNA hybrids offer a significant advantage over other DNA materials in that the UV absorbance of its DNA component is observable and not overshadowed by the optical properties of the polymer scaffold. This allows us to directly monitor the behavior of the DNA strands in the aggregate on a molecular level (i.e., single-stranded vs hybridized) rather than indirectly through the physical state of the overall assembly (aggregate vs dispersed).[21]

To evaluate the relative importance of aggregate dissolution vs short-range interduplex interactions in the melting behavior of polymer−DNA hybrids, we developed a system where short DNA strands could hybridize within an aggregate environment and then independently dehybridize without destroying the aggregate (Scheme 1). Specifically, two polymer−DNA hybrids were prepared (**polyDNA(T_{10}-I)** and **polyDNA(T_{10}-II)**) that contain a deca(thymidine) (**T_{10}**) spacer linking a 15 base-pair (bp) complementary sequence (**I** and **II**, respectively) to the polymer backbone. After these complementary polymer−DNA hybrids are hybridized together, the **T_{10}** spacers remain available for duplex formation with small, unmodified deca(adenosine) (**A_{10}**) strands. The resulting partially tethered **A_{10}:T_{10}** duplex has an inherently lower melting temperature than the fully tethered 15-mer **I**:**II** duplex and thus should dehybridize from the aggregated polymer−DNA:polymer−DNA hybrids (Scheme 1A) well below the melting transition of the latter (Scheme 1B).

Results and Discussion

Comb polymer−DNA hybrid precursors were synthesized according to our previous report.[9] Briefly, phosphoramidite-modified ROMP-based poly(norbornene) chains were coupled to oligonucleotide sequences comprised of the deca(thymidine) linker and complementary 15-base sequences to give **polyDNA-(T_{10}-I)** and **polyDNA(T_{10}-II)** as shown in Figure 1. Consistent with our earlier report,[9] when these polymer−DNA hybrids were combined in equal amounts in PBS buffer at room temperature, they formed duplex networks that exhibited a sharp melting transition around 60 °C (Figure 1A). We then prepared an **A_{10}** strand that could hybridize to the **T_{10}** spacer sequence while not being involved in maintaining the aggregate (Figure 1B). Due to the lower melting temperature (T_m) of the **A_{10}:T_{10}** duplex, these strands completely dissociate (Scheme 1A) well before the [**I**:**II**]-linked aggregate (Scheme 1B).

(11) Park, S. Y.; Stroud, D. *Phys. Rev. B* **2003**, *67*, 212202/1−212202/4.
(12) Kiang, C. H. *Physica A* **2003**, *321*, 164−169.
(13) Lukatsky, D. B.; Frenkel, D. *Phys. Rev. Lett.* **2004**, *92*, 068302/1-068302/4.
(14) Sun, Y.; Harris, N. C.; Kiang, C. H. *Physica A* **2005**, *354*, 1−9.
(15) Long, H.; Kudlay, A.; Schatz, G. C. *J. Phys. Chem. B* **2006**, *110*, 2918−2926.
(16) Lehn, J.-M. *Prog. Polym. Sci.* **2005**, *30*, 814−831.
(17) Yount, W. C.; Juwarker, H.; Craig, S. L. *J. Am. Chem. Soc.* **2003**, *125*, 15302−15303.
(18) Jin, R.; Wu, G.; Li, Z.; Mirkin, C. A.; Schatz, G. C. *J. Am. Chem. Soc.* **2003**, *125*, 1643−1654.
(19) Czlapinski, J. L.; Sheppard, T. L. *J. Am. Chem. Soc.* **2001**, *123*, 8618−8619.
(20) Li, X.; Liu, D. R. *Angew. Chem., Int. Ed.* **2004**, *43*, 4848−4870.
(21) Storhoff, J. J.; Lazarides, A. A.; Mucic, R. C.; Mirkin, C. A.; Letsinger, R. L.; Schatz, G. C. *J. Am. Chem. Soc.* **2000**, *122*, 4640−4650.

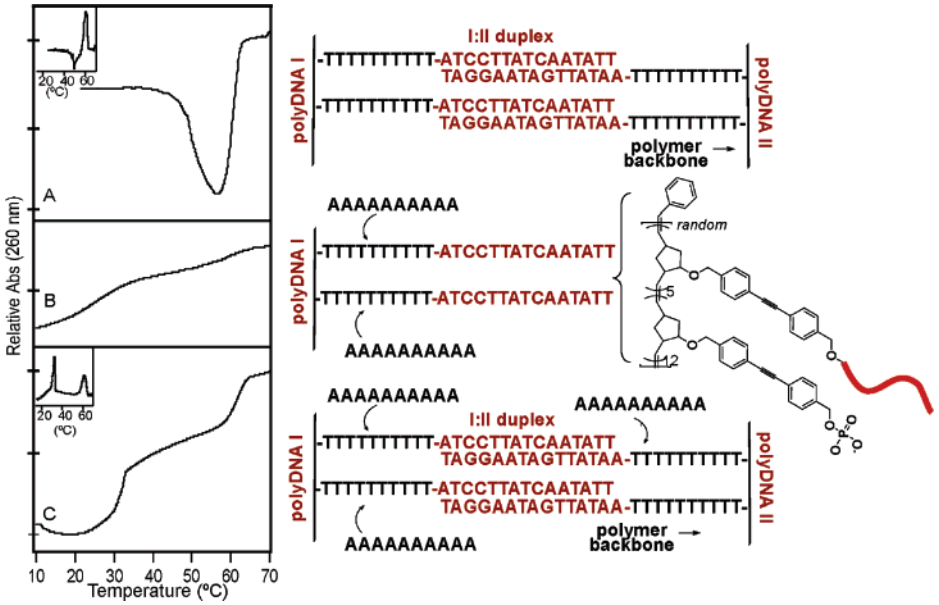

Figure 1. (Left) UV−vis absorbance melting profiles and (right) schemes illustrating the hydridization of (A) **polyDNA(T_{10}-I):polyDNA(T_{10}-II)** allowed to hybridize at room temperature overnight (the dip is typical and signifies aggregate restructuring),[22] (B) **polyDNA(T_{10}-I):A_{10}** allowed to hybridize at 10 °C overnight, and (C) **polyDNA(T_{10}-I):polyDNA(T_{10}-II):A_{10}** (1:1:2 mixture) allowed to hybridize at 55 °C for 8 h and then 10 °C overnight. Inset graphs inside the melting profiles are the corresponding smoothed first derivatives.

By combining the polymer−DNA hybrids **polyDNA(T_{10}-I)**: **polyDNA(T_{10}-II)** with unmodified A_{10} strands we could now observe how short DNA duplexes melt within an aggregate, as the aggregate remains intact. If the sharp melting relied only on the melting of the aggregate, the partially tethered A_{10}:T_{10} duplexes would not exhibit sharp transitions. However, if the neighboring-duplex interactions alone can induce cooperativity, the melting of the A_{10}:T_{10} duplex within the confined aggregate structure would be sharp.

PolyDNA(T_{10}-I), **polyDNA(T_{10}-II)**, and A_{10} (Figure 1A) were combined in a 1:1:2 ratio (relative to a total DNA strand concentration of 5.0 μM) in buffer (PBS = 10 mM, [NaCl] = 0.3 M, pH = 7) and allowed to anneal at 55 °C for at least 8 h. The mixture was then cooled to 10 °C and kept there overnight to allow the A_{10} and T_{10} sequences to hybridize. The melting of the hybridized mixture was subsequently monitored by UV−vis spectroscopy (λ_{max} = 260 nm for single-stranded DNA) as a function of temperature. We were delighted to observe a sharp melting transition for the partially tethered A_{10}:T_{10} duplex at 31 °C followed by a sharp transition for the polymer-linked **I**:**II** duplex dehybridization at 60 °C (Figure 1C). The first derivative of the melting profile exhibited two narrow peaks, indicative of two highly cooperative transitions distinct from each other. The presence of the sharp transition at 60 °C suggested that the [**I**:**II**]-linked aggregate was maintained during the initial sharp melting of the partially tethered A_{10}:T_{10} duplex. These results support that the presence of a "close-packed" duplex environment, not aggregate dissolution, is critical for inducing cooperativity (i.e., sharp melting) and that these two effects can be separated experimentally!

As shown in Figure 1B, only a broad transition around 25 °C is observed when **polyDNA(T_{10}-I)** is hybridized with A_{10} in the absence of **polyDNA(T_{10}-II)**. This experiment, where only one strand in the DNA duplex was tethered to the polymer, established that the duplexes must be rigidly held "close" to one another for cooperative neighboring-duplex interactions to occur, consistent with our previous report.[8]

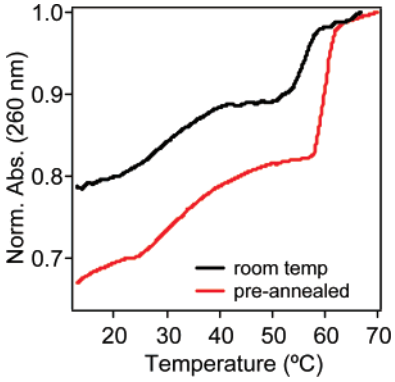

Figure 2. Black line: the UV−vis melting profile of the room temperature-hybridized **polyDNA(T_{10}-I):polyDNA(T_{10}-II):A_{10}** aggregate. Red line: the UV−vis melting profile associated with A_{10} that was added to a 55 °C pre-annealed **polyDNA(T_{10}-I):polyDNA(T_{10}-II)** aggregate mixture. The difference in absorbance between the two aggregate profiles is thought to result from increased hypochromicity in the annealed aggregate structure.[23]

It is interesting to note, however, that when **polyDNA(T_{10}-I)**, **polyDNA(T_{10}-II)**, and A_{10} were allowed to hybridize at room temperature (23 °C) instead of 55 °C, the UV−vis melting profile only displayed a broad transition in the A_{10}:T_{10} dissociation region (Figure 2, black line). Presumably the room-temperature aggregate, which is thought to be a low-density fractal structure containing fewer duplex interactions than an aggregate that has been annealed at high temperature,[22] does not force the A_{10}:T_{10} duplexes into close-neighbor proximity for cooperative melting. Similarly, when **polyDNA(T_{10}-I)** and **polyDNA(T_{10}-II)** were pre-annealed at high temperature (55 °C) prior to the introduction of A_{10}, the resulting aggregate

(22) Park, S. Y.; Lee, J.-S.; Georganopoulou, D. G.; Mirkin, C. A.; Schatz, G. C. *J. Phys. Chem. B* **2006**, *110*, 12673−12681.
(23) Purrello, R.; Raudino, A.; Scolaro, L. M.; Loisi, A.; Bellacchio, E.; Lauceri, R. *J. Phys. Chem. B* **2000**, *104*, 10900−10908.

Scheme 2. A Schematic Illustration of the Cooperative Melting of Neighboring $\mathbf{A_{10}}$ Strands (Green) That Share a Sodium Ion Cloud with Two Neighboring Duplexes Inside a Duplex-linked **polyDNA(T_{10}-I):polyDNA(T_{10}-II):A_{10}** Aggregate[a]

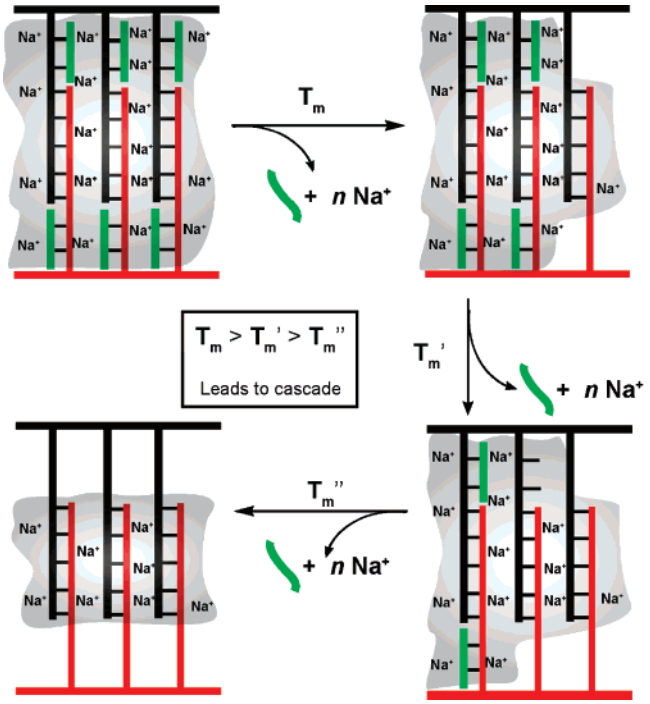

[a] The proximal conformation of the aggregated polymer−DNA hybrids leads to overlapping ion clouds.

displayed a broad transition in the $\mathbf{A_{10}}$:$\mathbf{T_{10}}$ melting region (Figure 2, red line). We postulate that this broad melting resulted from the slow diffusion of the $\mathbf{A_{10}}$ components into the pre-annealed dense network, leading to hybridization only at the less dense environment of the aggregate periphery.

Shared-Ion-Cloud Model. As our system possesses two different sharp melting transitions that can be separated experimentally, it can be used as the basis for a thermodynamic theory that would quantify the melting behavior observed in hybrid DNA materials containing mutually cooperative dissociations, with and without aggregate dissolution. Building upon the shared-ion-cloud model put forth by Jin et al.,[18] we refer to the **polyDNA(T_{10}-I):polyDNA(T_{10}-II):A_{10}** aggregate as *D*, so the initial dissociation of all of the partially tethered $\mathbf{A_{10}}$:$\mathbf{T_{10}}$ duplexes in this aggregate can be expressed in terms of the following equilibrium expressions:

$$
\begin{aligned}
&Q = [\mathrm{A}_{10}] && D_N \overset{K_N}{\rightleftharpoons} D_{N-1} + Q + nS \\
&S = [\mathrm{Na}^+] && \ldots \\
&n = \text{number of } \mathrm{Na}^+ \text{ ions released} && D_{N'+2} \overset{K_{N'+2}}{\rightleftharpoons} D_{N'+1} + Q + nS \\
&N = \text{number of cooperative steps} && D_{N'+1} \overset{K_{N'+1}}{\rightleftharpoons} D_{N'} + Q + nS
\end{aligned}
\qquad (1)
$$

where K_i represents the equilibrium constant for each step, D_N is the concentration of the fully hybridized aggregate (containing both the partially tethered $\mathbf{A_{10}}$:$\mathbf{T_{10}}$ duplexes at each end and the polymer-linked **I**:**II** duplex in the middle), and $D_{N'}$ represents the remaining aggregate with no $\mathbf{A_{10}}$:$\mathbf{T_{10}}$ duplexes but all of the polymer-linked **I**:**II** duplexes intact (Scheme 1). The number of steps *N* in the overall expression represents the cooperative unit, which corresponds to the number of duplexes with overlapping counterion clouds such that their equilibria are coupled (*vide supra*).[18]

The equilibrium constant for the first step (K_N) is assumed to be the smallest (i.e., it is less likely for the first dissociation to occur than the subsequent dissociations), which introduces cooperativity into our model.[18] This assumption is based on molecular dynamic simulations that suggest that a shared cation cloud is formed among closely associated DNA duplexes (within 5 nm).[15,24] As the first duplex of the fully hybridized aggregate (D_N) melts, the counterions associated with that duplex leave the shared-ion cloud, thereby decreasing the local salt concentration for the remaining duplexes (D_{N-1}). Because melting temperatures vary with the log of the salt concentration,[25,26] this decrease in the local salt concentration within the aggregate causes a decrease in the melting temperature of the remaining duplexes, resulting in a cascade melting effect (Scheme 2).

The dissociation of the polymer-linked **I**:**II** duplex can be explained in similar terms (eq 2). However, both sequences in the duplex are attached to the polymer, and therefore no untethered DNA ($\mathbf{A_{10}}$) is released when the aggregate melts.

$$
\begin{aligned}
&S = [\mathrm{Na}^+] && D_{N'} \overset{K'_{N'}}{\rightleftharpoons} D_{N'-1} + n'S \ldots \\
&n' = \text{number of } \mathrm{Na}^+ \text{ ions released} && D_2 \overset{K'_2}{\rightleftharpoons} D_1 + n'S \\
&N' = \text{number of cooperative steps} && D_1 \overset{K'_1}{\rightleftharpoons} D_0 + n'S
\end{aligned}
\qquad (2)
$$

The equilibrium constant for each individual step is K'_i, the number of cooperating duplexes in the second dissociation is N', and the corresponding number of cations released per step is n'. Here D_0 denotes the completely dissociated aggregate (Scheme 1B). Note that in this second step, it is also possible that aggregate/cluster melting can contribute to the melting curve. Methods for adding contributions from cluster melting to the model by Jin et al. are described elsewhere.[27] For our purpose of comparing the two transitions, these contributions, which would only affect the second melting transition, are neglected.

We can express the overall melting transition of our polymer−DNA hybrids in terms of *f*, the fraction of aggregate with dehybridized duplexes:

$$
f = \frac{xD_{N'} + D_0}{D_N + D_{N'} + D_0} = \frac{x + K'}{1 + \frac{1}{K} + K'} \qquad (3)
$$

where *x* is the fraction of the DNA that is single-stranded when the aggregate is in the $D_{N'}$ state, and *K* and *K*′ represent the overall equilibrium constants for the first and second melting transitions, respectively. *K* and *K*′ are also functions of the individual equilibrium constants corresponding to each step in the corresponding melting transitions: K_i and K'_i, respectively.[18] Incorporating the derived van't Hoff terms for K_i and K'_i into the functions for *K* and *K*′[18] and substituting the resulting expressions into eq 3 leads to the following:

(24) Long, H.; Schatz, G. C. *Mater. Res. Soc. Symp. Proc.* **2003**, *735*, C10.1.1.
(25) Krakauer, H.; Sturtevant, J. M. *Biopolymers* **1968**, *6*, 491−512.
(26) Record, M. T., Jr. *Biopolymers* **1967**, *5*, 975−992.
(27) Park, S. Y.; Gibbs-Davis, J. M.; Nguyen, S. T.; Schatz, G. C. *J. Phys. Chem. B* **2007**, *111*, 8785−8791.

$$f = \frac{x + \exp\left\{-\frac{\Delta H'}{R}\left(\frac{1}{T} - \frac{1}{T_m'}\right)\right\}}{1 + \exp\left\{\frac{\Delta H}{R}\left(\frac{1}{T} - \frac{1}{T_m}\right)\right\} + \exp\left\{-\frac{\Delta H'}{R}\left(\frac{1}{T} - \frac{1}{T_m'}\right)\right\}} \quad (4)$$

such that $\{\Delta H, T_m\}$ and $\{\Delta H', T_m'\}$ correspond to the first and the second dissociations, respectively. Prior to fitting eq 4 to our melting profile, we converted the temperature to kelvin, corrected for changes in DNA absorbance with temperature,[28,29] and then converted the profile to the fraction of dehybridized aggregate (f). The resulting fit yields ΔH and T_m values associated with both melting transitions.

Application of the Shared-Ion-Cloud Model to the Observed Melting Behavior. As shown in Figure 3, eq 4 fits well with our experimental data. The T_m and ΔH for the dissociation of partially tethered **A_{10}:T_{10}** duplex were found to be 304.2 K and 116 kcal/mol, respectively, while those for the melting of polymer-linked **I**:**II** were 334.7 K and 226 kcal/mol, respectively (Table 1, entry 1). For both of these aggregate-associated transitions, the ΔH and T_m values are larger than the values found for the melting of the DNA:polymer−DNA duplex with the same sequence (Table 1, entries 4 and 5).[30] However, the magnitude of the increase in ΔH is greater for the polymer-linked **I**:**II** duplex (Table 1, cf. entries 1 and 5) than the **A_{10}:T_{10}** pairs (Table 1, cf. entries 1 and 4). The larger change in ΔH observed for the **I**:**II** duplex compared with the **A_{10}:T_{10}** pair might be due to cluster melting effects not included in our model (*vide supra*) and/or an increased number of interacting duplexes in the **I**:**II** melting transition. Finally, the dehybridized fraction present when the aggregate was in the partially melted D_N state, x, was optimal at $x = 0.73$. This value of x is slightly higher than expected based on the number of base pairs that melt in the first and second transitions (20:15, calculated $x = 0.57$), suggesting that there is increased hypochromicity in the fully hybridized, annealed structure D_N.[23]

Interestingly, the room-temperature (Table 1, entry 3) and pre-annealed (Table 1, entry 2) aggregate both displayed higher melting temperatures than the **polyDNA(T_{10}-I):A_{10}** hybridization mixture (Table 1, entry 4). However, the breadth of the **A_{10}:T_{10}** melting transition in these experiments (based on the full width at half-maximum (fwhm) of the first derivative of the melting profile) are much larger than that for the annealed **polyDNA(T_{10}-I):polyDNA(T_{10})-II:A_{10}** (Table 1, entry 1), indicating little cooperativity. This increase in the melting temperature for the **A_{10}:T_{10}** duplex in all of the **polyDNA(T_{10}-I):polyDNA(T_{10})-II:A_{10}** systems, in comparison to the **polyDNAT_{10}-I:A_{10}** system, is similar to that observed in the analogous unmodified DNA experiment (see Figure S1 in the Supporting Information). The increased stabilization of the **A_{10}:T_{10}** duplex in the **T_{10}-I:T_{10}-II:A_{10}** nicked system compared to the same duplex in a system with only dangling (unhybridized) bases (**T_{10}-I:A_{10}**) can be attributed to better base stacking in the nicked system.[31]

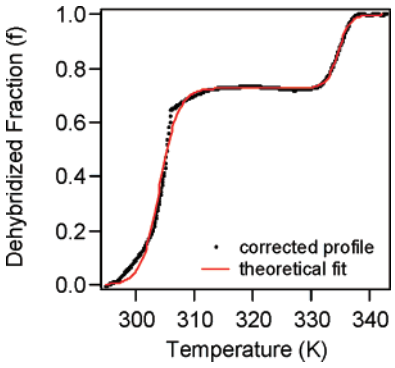

Figure 3. Fraction of single-stranded DNA f vs temperature in kelvin for the **polyDNA(T_{10})I:polyDNA(T_{10})II:A_{10}** aggregate. The fitted curve (dotted line) based on eq 4 shows excellent agreement with the corrected melting profile (solid line).

For the polymer-linked **I**:**II** duplex dehybridization, which leads to aggregate melting, slightly lower ΔH's were measured in the **polyDNA(T_{10}-I):polyDNA(T_{10})-II:A_{10}** annealed (Table 1, entry 1) and room-temperature (Table 1, entry 3) aggregates when compared with the **polyDNA(T_{10}-I):polyDNA(T_{10}-II)** aggregate (Table 1, entry 6) and the pre-annealed **polyDNA(T_{10}-I):polyDNA(T_{10})-II:A_{10}** aggregate (Table 1, entry 2). These slight depressions in the ΔH's could stem from the presence of the **A_{10}** strands during aggregate formation, which reduces the degrees of freedom around the **T_{10}** linkers. This in turn leads to a smaller number of interacting cooperative duplexes in the polymer-linked **I**:**II** duplex in comparison to hybridization mixtures without **A_{10}**. The less cooperative structures shown in entries 1 and 3 of Table 1 cannot rearrange to increase the overall cooperativity after the **A_{10}:T_{10}** duplexes dehybridize.

Determination of the Cooperative Unit. In our melting experiments, the cooperative unit N and N' corresponds to the number of duplexes that share an ion cloud and melt cooperatively. According to the original shared-ion-cloud theory by Jin et al., the melting cascade that led to sharp melting resulted in a complete loss of the condensed cation cloud.[18,24] Based on our dual-cooperative model, part of the cooperative ion cloud belonging to N' **A_{10}:T_{10}** duplexes can be disrupted while the ion cloud associated with N **I**:**II** duplexes remains intact (Scheme 2). Comparing the values of N and N' should elucidate how much alike are the cooperative environments in these two transitions and if they can have differing degrees of cooperativity despite their similar presence in the aggregate.

A useful first-order approximation for determining the number of cooperative duplexes can be ascertained from the ratio of the ΔH of the noncooperative hybridization mixture (i.e., polymer−DNA hybrid and the complementary unmodified DNA strand) and the ΔH of the cooperative system. Based on this ratio, the number of duplexes that collectively dehybridize in the partially tethered **A_{10}:T_{10}** melting transition (N) is approximately 2.1, whereas 3.1 duplexes melt cooperatively in the polymer-linked **I**:**II** transition (N') (Table 1, entry 1). Although not directly comparable, these values for the cooperative unit are on the order of the number of cooperative duplexes observed in the melting of DNA-modified gold nanoparticle aggregates ($N = 1.6$).[18] The difference in the cooperative unit for the **A_{10}:T_{10}** and **I**:**II** melting transitions in our experiment may reflect reorganization of the aggregate after the **A_{10}:T_{10}**

(28) Borer, P. N.; Dengler, B.; Tinoco, I., Jr.; Uhlenbeck, O. C. *J. Mol. Biol.* **1974**, *86*, 843−853.
(29) Marky, L. A.; Breslauer, K. J. *Biopolymers* **1987**, *26*, 1601−1620.
(30) Previously we found that the melting behavior of a DNA:polymer−DNA duplex was in fact very similar to that of the unmodified DNA:DNA duplex of the same sequence. See ref 8.
(31) Vasiliskov, V. A.; Prokopenko, D. V.; Mirzabekov, A. D. *Nucleic Acids Res.* **2001**, *29*, 2303−2313.

Table 1. Melting Temperatures (T_m), Full Width at Half-Maximum (FWHM) of the First Derivative of the Melting Transition and Changes in Melting Enthalpies (ΔH)

		A_{10}:T_{10}			I:II		
entry	hybridization mixture	T_m[a] (K)	FWHM (K)	ΔH[a] (kcal/mol)[c]	T_m[a] (K)	FWHM (K)	ΔH[a] (kcal/mol)
1	annealed **A_{10}**-inclusion aggregate[b] **polyDNA(T_{10}-I):polyDNA(T_{10})-II:A_{10}**	304.2	2.2	116	334.7	4.5	226
2	preannealed **A_{10}**-inclusion aggregate[c] **polyDNA(T_{10}-I):polyDNA(T_{10})-II:A_{10}**	306.0	11	62.4	333.2	3.3	300
3	room-temp **A_{10}**-inclusion aggregate[d] **polyDNA(T_{10}-I):polyDNA(T_{10})-II:A_{10}**	306.2	17	66.1	332.1	3.8	220
4	room-temp[d] **polyDNA(T_{10}-I):A_{10}**	299.3	16	56.3	--	--	--
5	room-temp[d] **DNA I:polyDNA(T_3-II)**[e,f]	--	--	--	318.0	11	72.7
6	room-temp aggregate[d] **polyDNA(T_{10}-I):polyDNA(T_{10}-II)**[f]	--	--	--	333.8	3.3	273

[a] All ΔH and T_m data were obtained by fitting eq 4 to the corresponding melting curves. [b]All three DNA components were annealed at 55 °C. [c]Complementary polyDNA were pre-annealed at 55 °C before introducing the A_{10}. [d]All components were hybridized at room temperature. [e]Melting profile data from ref 8. [f]The concentration of each DNA sequence is 1.9 μM.

melting transition, resulting in an increase in the number of **I**:**II** duplexes sharing a condensed ion cloud and/or different geometrical constraints imparted by the rigid polymer backbone. For the **polyDNA(T_{10}-I):polyDNA(T_{10}-II)** aggregate (Table 1, entry 6), the cooperative unit based on the ratio is 3.8, indicating that the presence of the **A_{10}** strands does decrease the number of cooperative duplexes in the resulting aggregate.

Conclusions

Our work clearly isolates contributions from neighboring-duplex interactions from the effects of aggregate dissolution in the melting of DNA duplexes in polymer−DNA:polymer−DNA aggregates. When short oligonucleotides are constrained to hybridize into a network that allows for optimal interduplex interactions, their melting transitions are significantly sharpened. However, this neighboring-duplex effect alone is not sufficient to account for the observed enhancement in melting transition for polymer−DNA:polymer−DNA hybrids. Other factors such as aggregate-phase behavior or multivalent interactions between polymer−DNA partners (akin to that observed for dendrimer−DNA hybrids[10]) also contribute. In other words, while neighboring-duplex interactions alone can lead to cooperative melting, the extent of stabilization observed in our polymer−DNA:polymer−DNA aggregates is a function of both neighboring-duplex interactions and other properties of our multiply linked polymer−DNA hybrid system. The combination of these effects leads to both increased T_m and sharp melting transitions as has been shown before.[8] Further delineation of these parameters may be obtained by investigating the effects of DNA strand orientation, polymer flexibility, and DNA number density on the melting behavior.

Our current work provides strong evidence that unmodified DNA in a highly dense, close-packed environment exhibits cooperative behavior. High cooperativity is a useful property for DNA-based systems, since it leads to switch-like transitions, which can be designed to trigger under very specific conditions. This improved understanding of the parameters that govern the cooperative and enhanced stability exhibited by materials such as our polymer−DNA aggregates could help in the design of other DNA-based materials. For example, surfaces modified with permanent DNA-based aggregates with appropriate interduplex spacing might exhibit high selectivity and increased binding constants with target DNA strands, thus improving the sensitivity of chip-based DNA detection. In addition, harnessing this cooperative behavior should lead to new opportunities in other systems that rely on DNA recognition events, such as DNA-templated ligation reactions[32] and DNA-based self-replication.[33,34]

Acknowledgment. Financial support by the NSF (DMR-0094347 to S.T.N., CHE-0550497 to G.C.S., and EEC-0647560 to both S.T.N. and G.C.S.), NIH-CCNE (NCI 1U54 CA119341-01 to both S.T.N. and G.C.S.), and AFOSR (DARPA DURINT to G.C.S.) is appreciated. We thank Professor Chad A. Mirkin for his insightful comments as well as for the use of the DNA synthesizer and the thermal equipment. We acknowledge the use of instruments in the Polymer Characterization Facility and the Analytical Services Laboratory at Northwestern University (both supported by the NSF-MRSEC and NSF-NSEC programs and the state of Illinois).

Supporting Information Available: Preparative procedures for hybridization mixtures, supplemental figures, and theoretical derivations. This material is available free of charge via the Internet at http://pubs.acs.org.

JA073034G

(32) Silverman, A. P.; Kool, E. T. *Chem. Rev.* **2006**, *106*, 3775−3789.
(33) Robertson, A.; Sinclair, A. J.; Philp, D. *Chem. Soc. Rev.* **2000**, *29*, 141−152.
(34) Ye, J.; Gat, Y.; Lynn, D. G. *Angew. Chem., Int. Ed.* **2000**, *39*, 3641−3643.